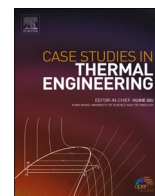




Contents lists available at ScienceDirect

Case Studies in Thermal Engineering

journal homepage: www.elsevier.com/locate/csite

Conventional and advanced exergoeconomic indicators of a nitric acid production plant concerning the cooling temperature in compression Train's intermediate stages

Ana Buelvas Hernández^a, Juan Gabriel Fajardo^b, Deibys Barreto^b,
Gaylord Enrique Carrillo Caballero^b, Yulineth Cárdenas Escorcía^{c,*},
Carlos Ramón Vidal Tovar^d, Yimy Gordon Hernández^e

^a Universidad Del Norte, Engineering Faculty, Mechanical Engineering Department, Barranquilla, Colombia

^b Universidad Tecnológica de Bolívar (UTB), Engineering Faculty, Grupo de Investigación EOLITO, Cartagena, Colombia

^c Energy Department, Universidad de la Costa (CUC), Grupo de Investigación GIOPEN, Barranquilla, Colombia

^d Universidad Popular del Cesar, Ingeniería Agroindustrial, Grupo de investigación CRECI, Valledupar, Colombia

^e Universidad Popular del Cesar, Comercio Internacional, Grupo de investigación FACEUPC, Valledupar, Colombia

ARTICLE INFO

Keywords:

Exergoeconomy
Endogenous exergy
Exogenous exergy
Avoidable exergy
Inevitable exergy
Exergo-economic indicators

ABSTRACT

In the refining and petrochemical industrial sector, large amounts of energy are used, so using the concept of exergy allows a rational use of this resource. In the different exergy and exergoeconomics studies applied in petrochemical plants, parameters of interest have been determined to evaluate the thermal efficiency, the potential for process improvement, the irreversibilities produced by the interaction between the components of the system and the operation of each one, and the energy costs associated with each of these irreversibilities. This paper presents an advanced exergy analysis and an exergo-economic analysis applied to a nitric acid production plant with an installed capacity of 350 metric tons per day, whose operating principle is based on the Ostwald method, and both the behavior of endogenous exergy destruction and the behavior of exogenous, avoidable and unavoidable exergy destruction are studied, exogenous, avoidable and unavoidable exergy destruction and the associated exergy costs in each of the heat transfer equipment and reactive equipment that make up the plant, about the cooling temperature in the intermediate stages of the compression train are studied using a mathematical model. The chemical reactions involved in the production process are the points of interest in the research of this work. Some of the results show that 54 % of the total exergy destruction can be recovered by intervening in the components. On the other hand, in the Catalytic Converter (CONV), it is convenient to consider the investment costs to reduce the exergy destruction costs. Similarly, in the Tail Gas Heater (TGH), it is beneficial to reduce the total investment to improve the process economics. On the other hand, the cost of exergy destruction of the plant resulted in 770.77 USD/h. In addition, it could be determined that the interactions between the components significantly affect the investment costs.

* Corresponding author.

E-mail addresses: buelvasana@uninorte.edu.co (A. Buelvas Hernández), jfajardo@utb.edu.co (J.G. Fajardo), dbarreto@utb.edu.co (D. Barreto), gcarrillo@utb.edu.co (G.E. Carrillo Caballero), ycardena6@cuc.edu.co (Y. Cárdenas Escorcía), carlosvidal@unicesar.edu.co (C.R. Vidal Tovar), yimygordon@unicesar.edu.co (Y. Gordon Hernández).

<https://doi.org/10.1016/j.csite.2021.101214>

Received 19 February 2021; Received in revised form 2 June 2021; Accepted 1 July 2021

Available online 30 July 2021

2214-157X/© 2021 The Authors. Published by Elsevier Ltd. This is an open access article under the CC BY license

(<http://creativecommons.org/licenses/by/4.0/>).

Nomenclature

\dot{E}_1	Exergy consumed (kW)
\dot{m}	Mass flow (Kg/s)
\dot{V}	Volumetric flow (m ³ /s)
v	Specific air volume (m ³ /kg)
T	Temperature (°C)
P	Press (KPa)
\dot{Q}	Heat transfer (kW)
\dot{Z}	Cost ratio associated with investment capital (\$/h)
c	Unit cost of exergy (\$/GJ)
r	Relative Cost Difference (%)
f	Exergoeconomic Factor (%)
i	Average inflation rate(%)
y^*	Percentage of exergy destruction (%)
\bar{x}	Mole fraction
e^{CH}	Specific chemical exergy (kJ/kg)
e^{PH}	Specific physical exergy (kJ/kg)
H	enthalpy
K	Equilibrium constant

Greek letters

ε	Eficiencia exergética (%)
η_s	Eficiencia isentrópica (%)
ε	Efectividad (%)
Δ	Delta

Subíndices

D	Destruction
F	Fuel
P	Product
R	Reactive
kth	k-eth plant component
tot	Total
OMC	Cost of operation and maintenance
Gibbs	Gibbs Free Energy
Reference state	Air
HN3	Ammonia

Superscripts

AV	Avoidable
UN	Inevitable
EX	Endogenous
EN	Exogenous
CI	Capital investment
OM	Operation and Maintenance

Abbreviations

CT	Compression train
ST	Steam Turbine
LPC	Low-pressure compressor
HPC	High-Pressure Compressor
IC	Inter-coolers
EXP	Expander
AF	Air filter
GM	Gas mixer
CONV	Catalytic Converter
AH	Air Heater
HRSG	Heat recovery boiler
PF	Platinum filter

TGH	Glue gas heater
TGTH	Glue gas temperature control unit
CC	Condenser
AS	Acid separator
ABS	Absorption tower
HR	Reagent Enthalpy
HP	Product Enthalpy

1. Introduction

Exergetic studies carried out in petrochemical plants with reactive systems show that the plant's greatest irreversibilities are concentrated mainly in the reactive equipment. It is essential to know the degree of energy degradation because there are uncontrollable factors such as climate change that affect energy generation. In this way, some existing and future power plants in certain regions will be affected by global climate change) [1]. In the industrial sectors of refining and petrochemicals, large amounts of energy are used, so using the concept of exergy allows fair use of life; in turn, its ability lies in considering the model of the three E's: energy-economy-ecology, where techniques based on exergy lead to reduce energy degradation in a technically feasible, cost-effective and environmentally sustainable. This technique also offers more detailed information on industrial processes' performance for their optimization and improvement [2]. When analyzing processes, the product obtained must be compared with the consumption or cost that has been necessary to get it. For this comparison to have a precise meaning, both concepts must be expressed in equivalent units (of equal thermodynamic value), which is achieved with the exergy [3]. Exergy-based analyses provide a quantitative measure of the inefficiency of a process [4]. In turn, exergoeconomics is a cost-effective tool that provides engineers with valuable information from energy conversion systems that cannot be obtained through conventional energy and economic models [5].

1.1. Conventional exergetic analysis

Exergetic indicators applied to oil refineries provide necessary performance measures to evaluate their potential for energy improvement. The purpose of an exergetic analysis applied to a crude oil distillation unit is to improve the efficiency of the process's energy utilization, both qualitatively and quantitatively [6]. The minimum and maximum exergetic efficiency values of a crude oil distillation unit were 51.2 % and 313670.11 MW, respectively. While the flash drum has an exergetic efficiency of 74.1 % and irreversibility of 1957-61.10 kW, for the furnace, these parameters are 75.1 % and 39259.06 kW, respectively. Once the exergetic evaluation was made, it was possible to deduce that the process's economic operation should consider the improvement of the performance of the crude distillation unit and should operate the process with a minimum number of trays [7]. Simultaneously, the total energy and exergetic efficiencies of a crude oil heating unit are 60.94 % and 19.34 %, respectively. Likewise, the highest exergy destruction rates occur in the solar field system, the thermal heating system, and the heat exchangers [8]. In turn, Nur et al. apply an exergetic analysis to a furnace and a crude oil preheating train of a crude oil distillation unit. The most significant exergy destruction occurs at the furnace entrance. The strategies proposed to improve the efficiency of the system were the reduction of heat loss from the furnace and the implementation of a cleaning plan for the preheating train. The cleaning program contributed 5.6 % of energy savings. However, with the reduction of heat loss from the furnace, approximately 6.4 % were obtained more significant cost savings. Exergetic analysis was applied to critical components such as condensers, furnaces, and distillation columns of a crude distillation unit. The locations and magnitudes of process inefficiency were detected according to the exergy loss distribution analysis. Compared to the primary process, the improved process's exergy efficiency increases from 28.9 % to 41.4 %, and total annual consumption is reduced by 28.7 % under the same flows and qualities of each product. The proposed framework can be extended to similar chemical separation processes to achieve more incredible energy and exergy savings [9].

A conventional exergetic analysis identifies thermodynamic inefficiencies by evaluating the destruction of exergy within each component. Care should be taken when using exergy destruction within a part when concluding the optimization of an energy system in general; this is because the exergy destruction that occurs within a component is not due exclusively to that component, but also the inefficiencies within the other details [10]. This means that two parts can represent the irreversibilities within the element of an energy conversion system: the first part depends on the irreversibilities within the system under consideration, unlike the second part, which refers to the inefficiencies within the remaining components of the system. These two concepts can also be called endogenous exergy destruction and exogenous exergy destruction respectively [10]; in addition to this, only a part of the exergy destruction in a component can be avoided (avoidable exergy destruction), taking into account that each member imposes several constraints including physical, technological and economic. Knowing the endogenous and exogenous exergy destruction together with the avoidable and unavoidable exergy destruction can provide a realistic measure of the optimization potential of an energy system [11]. This is what is known as advanced exergetic analysis.

1.2. Exergo-economic analysis

Some research related to exergo-economic analysis is presented below: Tock y Marechal [12] analyzes the thermochemical production of hydrogen and electricity from the implementation of lignocellulosic biomass, which also studies Caliendo et al. [13]. They explore through thermoeconomic models the combination of thermodynamics with economic analysis. On the other hand, Brown,

Gassner, Fuchino, y Maréchal [14], address the thermo-economic evaluation of a medium-scale plant (20 MW) that uses a wood gasification system; the relationship between total investment costs and the efficiency of exergy electricity production was obtained. Rivarolo et al. [15] focus the study on the evaluation and optimization of the thermodynamic and economic performance of the production of methanol from biomass through the application of integration techniques and process optimization. It was determined that the overall energy efficiencies are similar for the two configurations. Production costs remain well above the current price for natural gas-derived methanol and are strongly influenced by the estimated value of the gasification unit purchase price and biomass. Singh et al. [16] report the exergo-economic analysis of a milk production plant in India, showing both the overall exergetic efficiency and plant-specific exergy destruction, and the cost rate of exergy destruction for the entire plant not exceeding 3270.68 R/h. The higher value of the percentage relative cost difference was associated with a butter melter. Simultaneously, the exergo-economic factor revealed that the impact of the capital investment was more influential on the butter with a value of 8 %.

Abosoglu et al. [17] used exergy destruction cost ratios, the relative cost difference, and the exergo-economic factor for the analysis of all diesel cogeneration system components that allowed the identification of the elements with the most significant exergy destruction and those with the most tremendous potential for improvement. X. Zhang et al. [18] present and model a biogas and natural gas combined heat and power (CCHP) co-firing system based on a ground source heat pump using exergetic and exergonomic methods. The results indicate that natural gas injection improves energy efficiency, when the gas mass ratio varies from 0 to 1.0, the unit cost of electricity generated by the gas turbine, chilled water, and hot water decreases from \$11.26/GJ, \$92.21/GJ, and \$69.92/GJ to \$3.84/GJ, \$43.52/GJ and \$23.73/GJ, respectively.

The exergo-economic analysis of a gas turbine cycle is combined with a pressurized water reactor (PWR) power plant to increase overall plant efficiency. It was determined that an optimum pressure ratio exists for each gas turbine inlet temperature. The total combined cycle cost rate and specific cost of work produced for a gas turbine inlet temperature of 1500 K and a compressor pressure

Table 1
Advanced exergetic analysis research.

Title of the paper	Description	Research area	Year	References
Conventional and advanced exergy analysis of a geothermal-driven dual fluid Organic Rankine Cycle (ORC)	A conventional and advanced exergetic analysis is performed on the organic Rankine cycle of double geothermal fluid. The low-pressure steam generator (LPVG), the low-pressure turbine (LPT), and the high-pressure steam generator (HPVG) are the essential components for advanced exergy due to their considerable rates of avoidable endogenous exergy destruction.	Endogenous and exogenous exergetic analysis	2017	[23]
Advanced exergy analysis to evaluate the performance of a military aircraft turbojet engine (TJE) with an afterburner system: Divide exergy destruction into inevitable/avoidable and endogenous/exogenous	An advanced exergetic analysis is applied to an airplane turbojet, whose inevitable exergetic destruction rate is 93 % in MIL mode and 98 % in AB mode. Interactions between the components appear to be weak, with the endogenous exergy destruction rate being 83 % in MIL mode and 94 % in AB mode.	Endogenous and exogenous exergetic analysis	2017	[24]
Advanced exergy analysis for an anodic gas recirculation solid oxide fuel cell	An advanced exergy analysis for a solid oxide fuel cell with anode gas recirculation reveals the values of the first-level division of exergy destruction for all system components. 62 % of the total exergy destruction in the system is endogenous, and 38 % is exogenous. Also, 54 % of the total exergy destruction is avoidable and the rest, 46 %, is unavoidable.	Endogenous, exogenous, avoidable, and unavoidable exergetic analysis	2017	[25]
Conventional and advanced exergy analysis of an underwater compressed air energy storage system	A 2 MW underwater compressed air energy storage system (UWCAES) is subjected to conventional and advanced exergetic analysis. The final stage of the compressor is shown to have the most significant potential for improvement. The interactions between the system components are involved, but not very strong. Subsequently, the total exergetic efficiency does not necessarily increase as the performance of the individual parts improves.	Endogenous and exogenous exergetic analysis	2016	[26]
Analysis of the thermodynamic improvement potential of a selected cement manufacturing process: Advanced exergy analysis	An exergetic evaluation of a cement plant uses conventional and advanced exergetic analysis to determine the system. The main internal exergy losses were identified during the calcination process and the two departments of the crude oil processing plant, amounting to approximately 78.66 %, 70.86 %, and 72.12 %, respectively. The advanced analysis findings show that 15 %, 29.21 %, and 31.54 % of the total exergy destruction at calciner and wild plants 1 and 2, respectively, is avoidable.	Endogenous, exogenous, avoidable, and unavoidable exergetic analysis	2018	[27]

ratio of 13 were determined to be \$41,882/hr and \$31.63/MWh, respectively [19].

Fajardo et al. [20]. Developed an exergo-economic analysis of an agro-industrial wheat flour plant located in Cartagena and obtained a 95.08 % exergy destruction rate. The process's low overall exergetic efficiency was identified with a value of 0.257 %, which confirmed that the high exergetic destruction is typical of the process. The exergo-economic factor determined that an economic investment should be made that would be beneficial for the system Bin et al. [21] showed that as the gas turbine inlet air temperature decreases by 1 °C, the power generated and the thermal efficiency of the gas turbine increases by 0.53 % and 0.22 %, resulting in a 0.192 % increase in propane recovery, respectively when the gas turbine inlet air temperature cools from 40 °C to 15 °C (ISO condition), the propane production rate increases by 245 bbl/day. This corresponds to savings of \$18000/day. The resulting recovery period with the use of 100 % of the waste gas is 8.5 months, and the use of 20 % of the waste gas is 2.5 years.

1.3. Advanced exergetic analysis

An advanced exergetic analysis is applied to a nitric acid production plant with a capacity to process 350 tons/day with a concentration of 55 %. Where catalytic oxidation of ammonia, condensation, and absorption of nitrous gases are considered the primary process in nitric acid production. The destruction of exergy was 46772.55 kW. The most significant impact was the catalytic converter, which presented 75.1 % of the real avoidable exergy destruction rate of the plant [11]. While the avoidable and unavoidable exergy analysis of a fluidized bed coal burner (FBCC) and a heat recovery steam generator (HRSG) at a textile plant located at Torbalı, Izmir, have avoidable and unavoidable exergy destruction rates of 2999 kW and 760 kW as measured respectively. Consequently, exergy efficiencies were modified to 53.1 % and 48.1 %, respectively [22].

Table 1 describes five advanced exergetic studies conducted between 2016 and 2018, which study the behavior of endogenous, exogenous, avoidable, and inevitable exergetic destruction of different energy systems.

1.4. Advanced exergo-economic analysis

The advanced exergo-economic analysis allows determining the economic effects of the advanced factors of the exergetic analysis. In this way, the strategies for the reduction of total costs can be defined [28]. Under this scenario, Palizdar et al. [29] perform an advanced exergo-economic analysis of a small-scale dual nitrogen expansion process for LNG production, where it was observed that the compressors have the highest total costs; In contrast, most of the exergy destruction cost of the compressors and expanders are endogenous and avoidable, revealing a high potential for improvement. However, a high percentage of the investment cost of the equipment is inevitably endogenous. The most economically essential components are EXP-1 and EXP-2, with 59 % and 33 % of the total avoidable cost.

On the other hand, in an advanced exergo-economic analysis applied to three mixed refrigerant liquefaction processes, it was found that the exergy destruction cost of the compressors is avoidable. At the same time, heat exchangers and air coolers are unavoidable. The investment cost of heat exchangers and air coolers is avoidable, while compressors inevitable [30]. In turn, a Kalina cycle is solar-powered, and the absorber and pump are shown to have the highest and lowest exergy destruction cost rate, (\$1.3/hr and \$0.009/hr), respectively. The turbine and separator have the highest and lowest exergo-economic factor, (85.88 % and 1.105 %), respectively [31].

Similarly, analysis of a natural gas helium recovery process configuration and sensitivity analysis for exergonomic factors and exergy destruction cost of useful devices indicates that Heat Exchanger-105 and Heat Exchanger-104 have the highest exergy destruction cost at \$1889.68/hr and \$1263.58/hr, respectively. It is suggested that the exergy destruction cost of the compressors is avoidable. The exergy destruction costs induced by the remaining components are not significant, so the interactions between the process equipment are not strong [32].

A conventional and advanced exergo-economic analysis of a nitric acid production plant is carried out in this study. This plant comprises reactive and non-reactive equipment, whose transformation from ammonia to nitric acid is divided into two sections: (a) ammonia oxidation and (b) oxidation and absorption of nitrogen oxides. The reactive equipment used corresponds to a catalytic converter and an absorption tower where these two sections are carried out. While in the non-reactive equipment, there are heat exchangers, a cooler condenser, and a heat recovery boiler used to cool and heat the process gas, separate the weak acid and the process gas, and generate water vapor to take advantage of the heat content of the system respectively.

Exergetic studies carried out in petrochemical plants with reactive systems show that the significant irreversibilities of the plant are concentrated mainly in the reactive equipment. Simultaneously, the advanced exergetic analysis studies the behavior of the destruction of avoidable, inevitable, endogenous, and exogenous exergy. Still, it is not evident the variation of these parameters to the entrance temperature to the compressors and turbines of these plants. No system models were found that relate the costs of total irreversibilities to total production.

D. Barreto et al. [33] conducted research similar to this work and applied advanced exergy and exergy-economic analysis to improve energy and economic efficiency in an air-cooled steam injection gas turbine cycle power plant with a compression cooling machine. The results showed that the main sources of irreversibilities and higher costs are in the Combustion Chamber, the Heat Recovery Steam Generator, and the Gas Turbine. These last two components have the greatest potential for improvement and can be achieved by adjusting the overall system configuration because exogenous exergy destruction is avoidable to a more significant extent. In turn, they conclude that the highest investment costs can be reduced in the Combustion Chamber and the Gas Turbine. Whose main difference with the research of this work is that the nitric acid plant has more reactive systems, therefore, the effects of the chemical reactions are studied concerning the cooling temperature at the inlet of the compression train, while D. Barreto et al. [33] analyze the

influence of the inlet temperature on the power output of the steam injection gas turbine cycle power plant.

Based on the literature review of conventional and advanced exergoeconomic analysis, the methodology and results sections show how this research unfolds. The methodology section explains the nitric acid production process and the reactions involved, then the energy balance equations and the thermodynamic model are developed. Then the equations of the conventional exergy and exergy-economic analysis are described and finally the equations necessary for the advanced exergy and advanced exergy-economic analysis are developed to obtain the energy costs of each component of the system, the total cost of production and the variation of this parameter concerning the cooling temperature, the indicators used in the study for the conventional and advanced exergy analysis were fuel exergy, product exergy, exergy destruction, exergy efficiency, and exergy destruction ratio. And for the conventional and advanced exergy-economic analyses were investment cost ratio, operation and maintenance cost ratio, exergy-economic factor, relative cost difference, and unit exergy cost. Finally, in the results section, there is an exhaustive analysis of each of the indicators of the conventional and advanced exergy-economic and exergy-economic analysis obtained from the exergy balances previously mentioned in the methodology.

2. Methodology

2.1. Nitric acid production process

The first part of the process occurs initially in a mixing chamber where compressed air between 690 and 862 kPa and ammonia are mixed, then this mixture passes through a platinum-rhodium catalytic gauze at 927 °C inside the catalytic converter and, as a consequence, nitrous gases and water vapor are obtained at the outlet of the catalytic converter (CONV) as shown in Fig. 1. The mixing chamber is a fixed baffle type, made of 304 stainless steel. It has a capacity of 125,300 lb/hr and 8510 lb/hr, an operating temperature of 310 °C and 65 °C, and a working pressure of 800 kPa and 1241 kPa for air and ammonia respectively. While the catalytic gauze has a 0.003" wire diameter, with platinum-rhodium-palladium alloy 95-5-0, and the weight it supports during the process is between 250 and 300 lb ammonia/oz - day. This catalytic converter is a catalyst basket type manufactured with 347 stainless steel of circular geometry whose capacity does not exceed 133,800 br/hr and handles an operating pressure of 786 kPa (see Fig. 2).

The air used for this process comes from a centrifugal compressor connected to a compression train which delivers oil-free air at a temperature of 184 °C. The ammonia used is 99.8 % ammonia by weight and free of lead, iron, silica, arsenic, phosphorus, and other elements. In turn, the air-ammonium mixing process is explosive between 11% and 11.5 % of volume in ammonia at a pressure of 690 kPa. While the centrifugal compressor has a capacity of 40,000 CFM, whose pressure and discharge temperature are 827 kPa and 177 °C, respectively. The process gas leaving the catalytic converter passes through an air heater and is cooled to 650 °C, then enters the waste recovery boiler where saturated steam is generated at 1896 kPa, and the nitrous gases are cooled to 243 °C causing the oxidation of nitrogen monoxide to nitrogen dioxide in the process gas by releasing more heat; it is then cooled to 196 °C by heat transfer with the tail gas in the tail gas preheater.

From this point, the process gas enters the cooler condenser, and nitric acid formation begins with the oxidation of the nitrogen oxides below 49 °C at high pressure and with excess oxygen. Subsequently, the absorption process of the nitrogen oxides occurs, causing the formation of the weak acid. The weak acid and non-condensing gases are separated in an acid separator (AS) as shown in Fig. 1; the diluted acid is pumped into the absorption tower, and the process gas enters the bottom of the building at 47 °C and is absorbed in water forming nitric acid with a concentration of 56 %.

The cooler condenser has a tube and shell configuration made of zirconium and stainless steel. It has 133,800 lb/hr capacity, whose heat transfer surface is 7270 ft², and works with an inlet and outlet temperature of 126 °C and 43 °C, respectively. While the acid separator has a capacity of 24,200 lb/hr of a weak acid, it works with an operating pressure and temperature of 682 kPa and 43 °C respectively, and it is made of 430 stainless steel material.

After the process gas enters the bottom of the tower, the air is added to clarify the acid product by removing dissolved oxides, and oxygen is added to oxidize the nitrogen monoxide that is formed in the absorption process. The process gas passes in countercurrent with the feed water that enters the absorption tower and comes into contact with each of the 35 absorption plates generating nitric acid. The feed water used to obtain nitrogen dioxide is pure with a chloride content below one ppm. The chlorides are concentrated in the absorption tower where the nitric acid is concentrated between 21 % and 23 %. In this sense, the heat of the reaction is removed from each plate using cooling coils to cool water flows. In this aspect, the yellow and concentrated 56 % nitric acid exits through the bottom of the tower and undergoes a subsequent bleaching process to improve the aesthetics of the product. It is essential to mention that the absorption tower has a capacity of 109,600 lb/hr, handles an operating pressure and temperature of 682 kPa, and 43 °C respectively, and has 316 cooling coils. The cooling water used comes from the plant's storage pool; this water is filtered in anthracite sand filters before entering the cooling tower pool, consisting of three circulation pumps. Two work continuously to maintain a

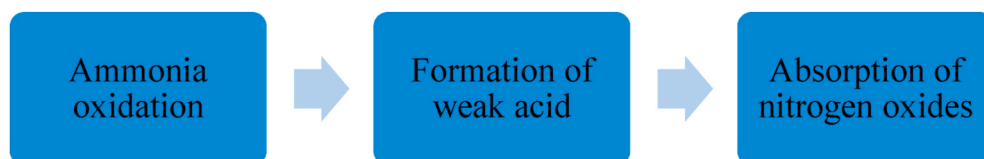


Fig. 1. Main stages of the nitric acid production process.

minimum recirculation volume of 8600 GPM.

Once the nitric acid production process is complete, the tail gas leaving the absorption tower passes through temperature control and tail gas pre-heater to increase its temperature from 40 °C to 593 °C. Its heat energy is recovered in the connected expander, which is connected to the centrifugal compressor as mechanical energy before it reaches the heat recovery system for the steam system. To this effect, the work done by the expander reduces the energy requirements of the compressor and therefore, the steam consumption of the Terry turbine. The expander is a gas turbine manufactured from carbon steel with a power of 7540 BHP, has a gas flow capacity of 138,200 lb/hr, works with an inlet, and outlet temperature of 593 °C and 296 °C, respectively, with a maximum inlet pressure of 862 kPa. At the same time, the Terry turbine handles a full power of 1800 HP and 6850 ppm.

2.2. Main chemical reactions generated in the process

In the process of ammonia oxidation within the CONV the following reaction occurs (Equation (1)) [11]:



On the other hand, reaction balances originate during nitrogen monoxide oxidation and weak acid formation in the CC, as shown in Equations (2) and (3) [11]:



2.3. Energy balance and thermodynamic model

The energy balance between two specified points of the process is applied at the entry and exit points of each plant component, the scheme of which is shown in Fig. 2. This energy balance (Equation (4)) assumes that the gases' behavior is ideal at all points of the process, the kinetic and potential energies are neglected, are not considered mass losses, and the components of the system analyzed are in a stable state [34].

$$\sum \dot{m}_{in}h_{in} + \dot{Q}_{in} + \dot{W}_{in} = \sum \dot{m}_{out}h_{out} + \dot{Q}_{out} + \dot{W}_{out} \tag{4}$$

Below is the model used to evaluate the total production of the plant concerning the moles of the gases resulting from the chemical reactions presented during the process.

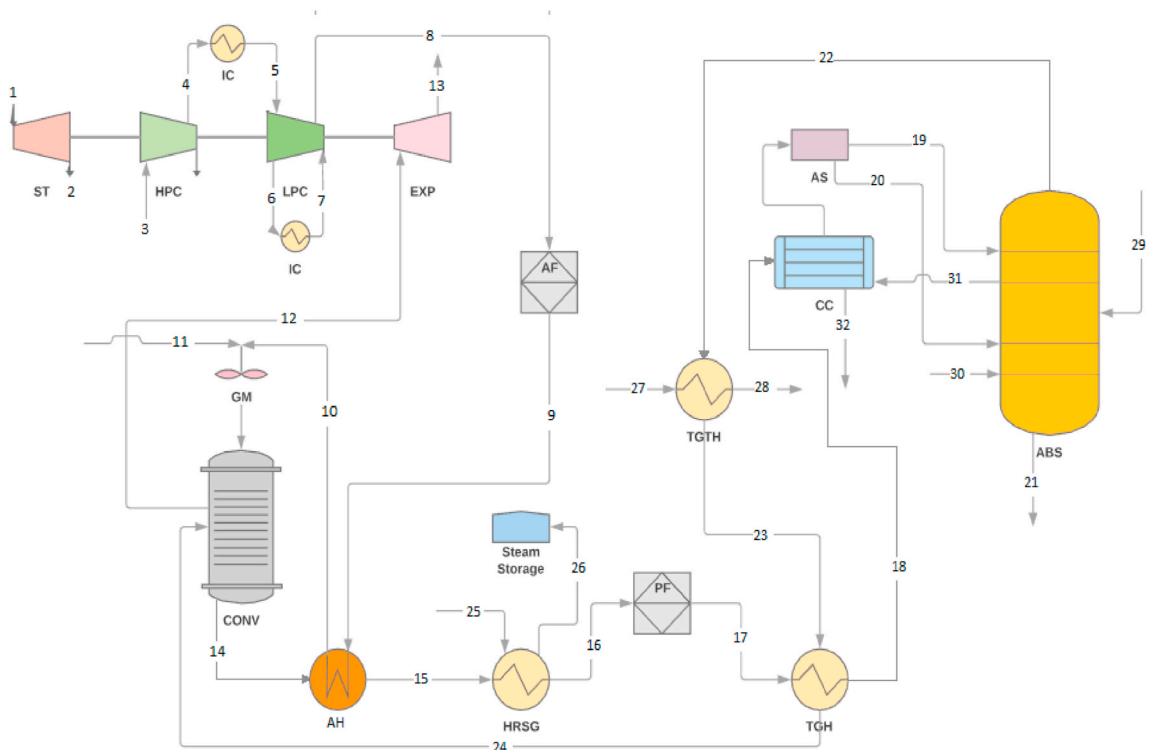


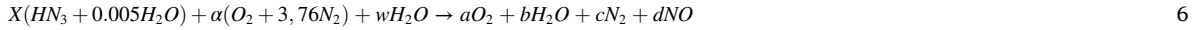
Fig. 2. Nitric acid production plant process diagram.

The model starts with the decrease of temperature in the intermediate stages of the TC, causing the increase of the air mass flow. The air density presents an inverse relation with the weather. The mass flow is calculated with equation (5) [34].

$$\dot{m}_{Air} = \frac{\dot{V}_{Air}}{v} \text{ (kg / s)} \quad 5$$

Once the air leaves the TC, the first combustion process occurs inside the CONV, while the second and third combustion processes are formed at the output of the CC and inside the ABS respectively. The combustion process in the CONV, CC, and ABS follows reactive systems analysis based on the first law for stationary flows.

The reagents and products of the combustion equation formed inside the CONV are in a molar base. The moles of the products are obtained through the balance of moles (Equations (7)–(9)) H, O, N, also through an equation of NO formation (Equation (10)) and through a complementary equation (Equation (11)) of the simultaneous reaction of chemical equilibrium for the construction of NO. The molar-based combustion equation formed within the CONV is defined by (Equation (6)) [35]:



To X , α and w The moles of ammonia, the moles of excess air, and the moles of steam, respectively, are represented. Y a , b , c , d represent the moles of each species present in the reaction products in the CONV.

$$\text{Balance Sheet of N : } X + 7,5\alpha \rightarrow 2c + d \quad 7$$

$$\text{Balance Sheet of H : } 3,01X + 2w \rightarrow 2b + d \quad 8$$

$$\text{Balance Sheet of O : } 0,005X + 2\alpha + w \rightarrow 2a + b + d \quad 9$$

$$\text{Training of NO : } \frac{1}{2}N_2 + \frac{1}{2}O_2 \rightarrow NO \quad 10$$

$$\text{The equilibrium constant NO [35] : } K_{PNO} = \frac{d^{V_{NO}}}{c^{V_{N_2}} b^{V_{O_2}}} \left(\frac{P}{N_{Totales}} \right)^{V_{NO} - V_{O_2} - V_{N_2}} \quad 11$$

To $V_{NO} = 1$, $V_{O_2} = 1/2$ y $V_{N_2} = 1/2$ [35], and the equilibrium constant for the simultaneous formation equation are calculated by equation (12) [35]:

$$\ln(K_{PNO}) = \frac{-\Delta Gibbs^*_{NO}(T_{Prod})}{R_u T_{Prod}} \quad 12$$

The fuel-air ratio (FAR) of the combustion process that is formed in the NOC is defined as follows (Equation (13)) [34]:

$$\lambda = \frac{\dot{m}_{HN_3}}{\dot{m}_{aire}} \quad 13$$

The gases produced by the CONV enter the heat exchanger network until they reach DC. The moles of the reagents formed at the outlet of the CC correspond to the moles of the products leaving the CONV and the moles of the products at the outlet of the CC are obtained through the balance of moles present in the chemical reaction (Equations (15)–(17)) H , O , N , two complementary equations of simultaneous reaction and two equations of chemical equilibrium for NO_2 y HNO_3 (Equations (18) and (21)). The equilibrium constants of the complementary equations of simultaneous chemical equilibrium reaction for the formation of NO_2 to calculate using equations (19) and (20) and the corresponding HNO_3 are calculated using equations (22) and (23). An energy loss on combustion of 2 % of the energy supplied by the reagents is predicted as recommended by Tsatsaronis [4]. The combustion equation used to obtain the moles of the products leaving the CC corresponds to (Equation (14)) [36]:



where e , f , g , h , y , j represent the moles of each species present in the reaction products.

$$\text{Balance Sheet N : } d + 7,53\alpha \rightarrow 2f + g + h + i \quad 15$$

$$\text{Balance Sheet H : } 2b \rightarrow i + 2j \quad 16$$

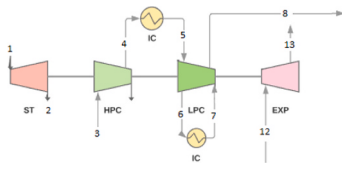
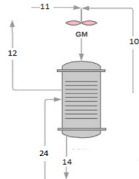
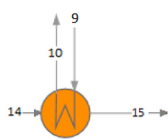
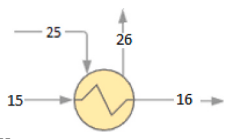
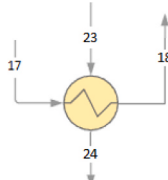
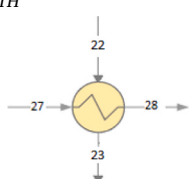
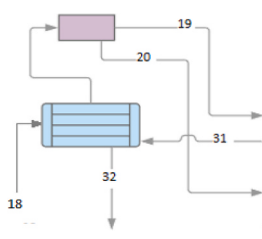
$$\text{Balance Sheet O : } d + 2\alpha + b \rightarrow 2e + 2g + h + 3i + j \quad 17$$

$$\text{Formation of } NO_2 : 2NO + O_2 \rightarrow 2NO_2 \quad 18$$

$$\text{Equilibrium constant } NO_2 [35] : K_{PNO_2} = \frac{h^{V_{NO_2}}}{f^{V_{NO}} e^{V_{O_2}}} \left(\frac{P}{N_{Totales}} \right)^{V_{NO_2} - V_{NO} - V_{O_2}} \quad 19$$

To $V_{NO_2} = 2$, $V_{NO} = 2$, y $V_{O_2} = 1$ [35], and the equilibrium constant for equation (18) of simultaneous NO_2 are calculated with Equation (20) [35]:

Table 2
Energy balance of each component of the nitric acid production plant.

Component	Energy balance
<p>CT</p> 	$\dot{Q}_{CT} = \dot{m}_1(h_1 - h_2) + \dot{m}_{12}(h_{12} - h_{13}) - \dot{m}_3(h_4 - h_3) - \dot{m}_5(h_8 - h_7 + h_6 - h_5)$
<p>CONV</p> 	$\dot{Q}_{CONV} = \dot{m}_{14}h_{14} + \dot{m}_{12}h_{12} - \dot{m}_{11}h_{11} - \dot{m}_{10}h_{10} - \dot{m}_{24}h_{24}$
<p>AH</p> 	$\dot{Q}_{AH} = \dot{m}_9(h_{10} - h_9) - (\dot{m}_{14}h_{14} - \dot{m}_{15}h_{15})$
<p>HRSRG</p> 	$\dot{Q}_{HRSRG} = \dot{m}_{25}(h_{26} - h_{25}) - (\dot{m}_{15}h_{15} - \dot{m}_{16}h_{16})$
<p>TGH</p> 	$\dot{Q}_{TGH} = \dot{m}_{24}(h_{24} - h_{23}) - (\dot{m}_{17}h_{17} - \dot{m}_{18}h_{18})$
<p>TGTH</p> 	$\dot{Q}_{TGTH} = \dot{m}_{23}(h_{23} - h_{22}) - (\dot{m}_{27}h_{27} - \dot{m}_{28}h_{28})$
<p>CC</p> 	$\dot{Q}_{CC} = \dot{m}_{18}h_{18} + \dot{m}_{31}h_{31} - \dot{m}_{19}h_{19} - \dot{m}_{20}h_{20} - \dot{m}_{32}h_{32}$
	$\dot{Q}_{ABS} = \dot{m}_{19}h_{19} + \dot{m}_{20}h_{20} + \dot{m}_{29}h_{29} + \dot{m}_{30}h_{30} - \dot{m}_{21}h_{21} - \dot{m}_{22}h_{22} - \dot{m}_{31}h_{31}$

(continued on next page)

Table 2 (continued)

Component	Energy balance
ABS	

$$\ln(K_{PNO_2}) = \frac{-\Delta Gibbs^*_{NO_2}(T_{Prod})}{R_u T_{Prod}} \quad 20$$



$$\text{Equilibrium constant } HNO_3 \text{ [35]: } K_{PHNO_3} = \frac{i^{V_{HNO_3}}}{g^{V_{NO_2}} j^{V_{H_2O}}} \left(\frac{P}{N_{Totales}} \right)^{V_{HNO_3} - V_{NO_2} - V_{H_2O}} \quad 22$$

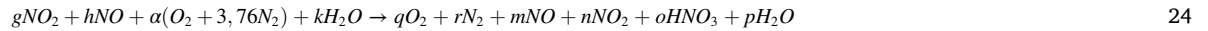
To $V_{HNO_3} = 2$, $V_{NO_2} = 3$, and $V_{H_2O} = 1$ [35] and the equilibrium constant for equation (3) 18 of simultaneous formation of HNO_3 is calculated with Equation (23) [35]:

$$\ln(K_{PHNO_3}) = \frac{-\Delta Gibbs^*_{HNO_3}(T_{Prod})}{R_u T_{Prod}} \quad 23$$

In this way, the DC output products enter the ABS, and the weak acid (HNO_3) is pumped into the absorption column. At the same time, the process gas (NO_2 , NO , O_2 , N_2) is introduced at the bottom of the absorption column to be absorbed by water to form nitric acid.

The moles of the products inside the ABS are obtained by the balance of moles present in the chemical reaction (Equations (25)–(27)) H , O , N , and two complementary equations of simultaneous chemical equilibrium reaction for the formation of NO_2 and HNO_3 (Equations (28) and (31)). The equilibrium constants of the complementary equations of the simultaneous reaction of chemical equilibrium for the construction of NO_2 are calculated using equations (29) and (30). The corresponding ones for HNO_3 are calculated using equations (32) and (33). A loss of energy in the combustion of 2 % of the energy supplied by the reagents is foreseen [4].

The combustion equation that models the number of moles coming out of the ABS is the following (Equation (24)) [35]:



$$\text{Balance of } N : g + h + 7,52\alpha \rightarrow 2r + m + n + o \quad 25$$

$$\text{Balance of } H : 2k \rightarrow o + 2p \quad 26$$

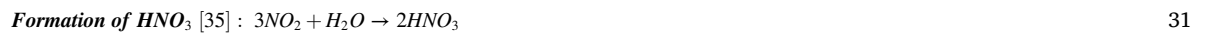
$$\text{Balance of } O : 2g + h + 2\alpha + k \rightarrow 2q + m + 2n + 3o + p \quad 27$$



$$\text{Equilibrium constant } NO_2 \text{ [35]: } K_{PNO_2} = \frac{n^{V_{NO_2}}}{m^{V_{NO}} q^{V_{O_2}}} \left(\frac{P}{N_{Totales}} \right)^{V_{NO_2} - V_{NO} - V_{O_2}} \quad 29$$

To $V_{NO_2} = 2$, $V_{NO} = 2$, y $V_{O_2} = 1$ [35], and the equilibrium constant for equation (18) of simultaneous NO_2 are calculated as (Equation (30)) [35]:

$$\ln(K_{PNO_2}) = \frac{-\Delta Gibbs^*_{NO_2}(T_{Prod})}{R_u T_{Prod}} \quad 30$$



$$\text{Equilibrium constant } HNO_3 \text{ [35]: } K_{PHNO_3} = \frac{o^{V_{HNO_3}}}{n^{V_{NO_2}} p^{V_{H_2O}}} \left(\frac{P}{N_{Totales}} \right)^{V_{HNO_3} - V_{NO_2} - V_{H_2O}} \quad 32$$

To $V_{HNO_3} = 2$, $V_{NO_2} = 3$ y $V_{H_2O} = 1$ y the equilibrium constant for equation (3) 18 of simultaneous HNO_3 is calculated by equation

(33) [35]:

$$\ln(K_{PHNO_3}) = \frac{-\Delta Gibbs^*_{HNO_3}(T_{Prod})}{R_u T_{Prod}} \tag{33}$$

Table 2 shows the energy balances for each of the components of the nitric acid production plant.

2.4. Conventional exergetic and exergonomic analysis

Equation (34) models the balance of exergy applied to each of the plant components. To do this, the desired outputs (product) and inputs required (fuel) in each of them are defined [11].

$$\dot{E}_{D,k} = \dot{E}_{F,k} - \dot{E}_{P,k} (kW) \tag{34}$$

Kinetic and potential energy are neglected because the values are minimal, therefore in the total exergy ratio \dot{E}_k , only the exigencies of physical character intervene (\dot{E}_k^{PH}) and chemical (\dot{E}_k^{CH}), which is expressed as follows in equation (35) [10]:

$$\dot{E}_k = \dot{E}_k^{PH} + \dot{E}_k^{CH} (kW) \tag{35}$$

The specific physical exergy for pure substances is obtained from equation (36) [34]:

$$e_k^{PH} = h_i - h_0 - T_0(s_i - s_0) \tag{36}$$

Specific chemical exergy is obtained using equation (37), where chemical exergies \bar{e}^{CH} molars of each compound are obtained from [35], Ref. [37].

$$\bar{e}^{CH} = \bar{x}_i \bar{e}_k^{CH} + RT_0 \sum \bar{x}_i \ln(\bar{x}_i) \tag{37}$$

The exergetic indicators used in the analysis of each component are exergetic efficiency and the exergetic destruction ratio through equation (38) and equation (39) respectively [18].

$$\epsilon_k = \frac{\dot{E}_{P,k}}{\dot{E}_{F,k}} (\%) \tag{38}$$

$$y_k^* = \frac{\dot{E}_{D,k}}{\dot{E}_{D,Total}} (\%) \tag{39}$$

In Table 3, the exergy of fuel and product for each component of the plant is established to obtain the irreversibilities later.

For each plant component, the balance of costs is applied as shown in Equation (40) [29], where $\dot{C}_{F,k}$ refers to the cost rate associated with fuel exergy, $\dot{C}_{P,k}$ is the cost rate associated with product exergy. At the same time, \dot{Z}_k^{CI} y $\dot{Z}_k^{O\&M}$ denotes the capital investment cost rate and the operating and maintenance cost rate of the component respectively [38]. The sum of these last two terms is what is denoted as \dot{Z}_k .

$$\dot{C}_{P,k} = \dot{C}_{F,k} + \dot{Z}_k^{CI} + \dot{Z}_k^{O\&M} (\$/h) \tag{40}$$

The cost rate associated with fuel exergy $\dot{C}_{F,k}$, and the cost rate associated with product exergy $\dot{C}_{P,k}$ are calculated using equations (41) and (42), respectively [20].

$$\dot{C}_{F,k} = \dot{c}_{F,k} \dot{E}_F (\$/h) \tag{41}$$

Table 3
Fuel Exergy and Product Exergy Equations for each plant equipment.

Component	Exergy of fuel	Product Exergy
CT	$\dot{E}_F = \dot{E}_1 - \dot{E}_2 + \dot{E}_{12} - \dot{E}_{13}$	$\dot{E}_P = \dot{E}_4 - \dot{E}_3 + \dot{E}_8 - \dot{E}_7 + \dot{E}_6 - \dot{E}_5$
CONV	$\dot{E}_F = \dot{E}_{10} - \dot{E}_{11} + \dot{E}_{24} + \dot{E}_{Q,conv}$	$\dot{E}_P = \dot{E}_{12} + \dot{E}_{14}$
AH	$\dot{E}_F = \dot{E}_{14} - \dot{E}_{15}$	$\dot{E}_P = \dot{E}_{10} - \dot{E}_9$
HRSG	$\dot{E}_F = \dot{E}_{15} - \dot{E}_{16}$	$\dot{E}_P = \dot{E}_{26} - \dot{E}_{25}$
TGH	$\dot{E}_F = \dot{E}_{17} - \dot{E}_{18}$	$\dot{E}_P = \dot{E}_{24} - \dot{E}_{23}$
TGTH	$\dot{E}_F = \dot{E}_{27} - \dot{E}_{28}$	$\dot{E}_P = \dot{E}_{23} - \dot{E}_{22}$
CC	$\dot{E}_F = \dot{E}_{18} + \dot{E}_{31}$	$\dot{E}_P = \dot{E}_{19} + \dot{E}_{20} + \dot{E}_{32}$
ABS	$\dot{E}_F = \dot{E}_{19} + \dot{E}_{20} + \dot{E}_{29} - \dot{E}_{30}$	$\dot{E}_P = \dot{E}_{21} + \dot{E}_{22} + \dot{E}_{31}$

$$\dot{C}_{P,k} = \dot{c}_{P,k} \dot{E}_P (\$/h) \tag{42}$$

While the capital investment cost rate Z_k^{CI} and the operation and maintenance cost rate $Z_k^{O\&M}$ by component are calculated using equations (43) and (44) [17].

$$Z_k^{CI} = \frac{PEC \left[\frac{i_r(1+i_r)^{n_r}}{(1+i_r)^{n_r} - 1} \right]}{3600(RTY)} (\$/h) \tag{43}$$

$$Z_k^{O\&M} = \frac{C_{Total}^{O\&M} PEC_k}{3600(RTY) \sum PEC_k} (\$/h) \tag{44}$$

The exergo-economic indicators applied to each component of the plant are The cost of destruction of exergy, the relative cost difference, and the exergo-economic factor [4]. Considering that product costs are fixed in each component, the value of exergy destruction is expressed by equation (45) [17].

$$\dot{C}_D = \dot{c}_{F,k} \dot{E}_{D,k} (\$/h) \tag{45}$$

The relative cost difference expresses the relative increase in the average cost per unit of exergy between the inputs and outputs of each of the components using equation (46) [17]:

$$r_k = \frac{c_{P,k} - c_{F,k}}{c_{F,k}} \tag{46}$$

The exergo-economic factor defines the relationship between non-relative costs and the total cost of a component. If the exergo-economic factor is small, the efficiency of the equipment must be improved; if the value is large, the investment capital must be decreased by purchasing the equipment [29]. This parameter is defined as shown in equation (47):

$$f_k = \frac{\dot{Z}_k}{\dot{Z}_k + \dot{C}_D} (\%) \tag{47}$$

The factor is usually between 35 % and 75 % for compressors and turbines [39].

Table 4 shows the cost balances and auxiliary equations for each component of the nitric acid production plant. The additional equations are derived from the configuration of the system components.

Table 4
Balance of cost equations and auxiliary equations for plant component.

Component	Balance of costs and auxiliary equations
CT	$\dot{C}_4 - \dot{C}_3 + \dot{C}_8 - \dot{C}_7 + \dot{C}_6 - \dot{C}_5 = \dot{C}_1 - \dot{C}_2 + \dot{C}_{12} - \dot{C}_{13} + \dot{Z}_{CT}$ $\frac{\dot{C}_1}{\dot{E}_1} = \frac{\dot{C}_2}{\dot{E}_2}$ $\dot{c}_1 = 0$ $\frac{\dot{C}_{12}}{\dot{E}_{12}} = \frac{\dot{C}_{13}}{\dot{E}_{13}}$
CONV	$\frac{\dot{E}_{12}}{\dot{C}_{12}} + \frac{\dot{E}_{13}}{\dot{C}_{14}} = \dot{C}_{10} - \dot{C}_{11} + \dot{C}_{24} + \dot{C}_{Q,conv} + \dot{Z}_{CONV}$ $\dot{c}_{12,11} = \dot{c}_{12} + \left(\frac{\dot{C}_{10}}{\dot{C}_{11}}\right)(\dot{c}_{12} - \dot{c}_{10})$
AH	$\dot{C}_{10} - \dot{C}_9 = \dot{C}_{14} - \dot{C}_{15} + \dot{Z}_{AH}$ $\frac{\dot{C}_{14}}{\dot{E}_{14}} = \frac{\dot{C}_{15}}{\dot{E}_{15}}$
HRSG	$\dot{C}_{26} - \dot{C}_{25} = \dot{C}_{15} - \dot{C}_{16} + \dot{Z}_{HRSG}$ $\frac{\dot{C}_{16}}{\dot{E}_{16}} = \frac{\dot{C}_{15}}{\dot{E}_{15}}$
TGH	$\dot{C}_{24} - \dot{C}_{23} = \dot{C}_{17} - \dot{C}_{18} + \dot{Z}_{TGH}$ $\frac{\dot{C}_{18}}{\dot{E}_{18}} = \frac{\dot{C}_{17}}{\dot{E}_{17}}$
TGTH	$\dot{C}_{23} - \dot{C}_{22} = \dot{C}_{27} - \dot{C}_{28} + \dot{Z}_{TGTH}$ $\frac{\dot{C}_{23}}{\dot{E}_{23}} = \frac{\dot{C}_{22}}{\dot{E}_{22}}$
CC	$\dot{C}_{19} + \dot{C}_{20} + \dot{C}_{32} = \dot{C}_{18} + \dot{C}_{31} + \dot{Z}_{CC}$ $\frac{\dot{C}_{32}}{\dot{E}_{32}} = \frac{\dot{C}_{31}}{\dot{E}_{31}}$
ABS	$\dot{C}_{21} + \dot{C}_{31} + \dot{C}_{31} = \dot{C}_{19} + \dot{C}_{20} + \dot{C}_{29} - \dot{C}_{30} + \dot{Z}_{ABS}$ $\frac{\dot{C}_{30}}{\dot{E}_{30}} = \frac{\dot{C}_{31}}{\dot{E}_{31}}$

2.5. Advanced exergetic and exergo-economic analysis

Advanced exergetic analysis can provide additional information to conventional exergetic analysis to improve the design and operation of energy conversion systems [40].

2.5.1. Destruction of endogenous and exogenous exergy

To consider the interactions between the components of a system, Tsatsaronis introduces the concept of the destruction of endogenous and exogenous exergy associated with the k-th part of a system (Equation (48)) [41].

$$\dot{E}_{D,k} = \dot{E}_{D,k}^{EN} + \dot{E}_{D,k}^{EX} \tag{48}$$

The destruction of endogenous exergy associated with the k-component $\dot{E}_{D,k}^{EN}$ is the part of the exergy destroyed within the same component that could appear when all the features operate ideally. The k-th segment operates with its real exergetic efficiency. The destruction of exogenous exergy $\dot{E}_{D,k}^{EX}$ is simultaneously due to the inefficiencies of the k-component and the inefficiencies of the other components. To determine these components, a model is elaborated that allows assessing the destruction of endogenous exergy of the k-component, in which all the parts of the plant operate with a 100 % energy efficiency, except the k-component that works with its real energy efficiency. The determination of exogenous and endogenous exergy destruction in a k-component indicates how to optimize that component and the whole system [41].

2.5.2. Destruction of inevitable and avoidable exergy

Due to technical, economical, and manufacturing method limitations, each component may have better thermodynamic behavior, which determines the inevitable part of exergy destruction. Within the different operational conditions that can be had for an element, the inevitable processes are established, to obtain the relation $(\dot{E}_D/\dot{E}_P)_k^{UN}$ for the component. With its best condition within the different operational conditions, it is possible to calculate the destruction of exergy inevitable in a real process. The reason for exergy destruction \dot{E}_D associated with the k-th component (Equation (49)) of a thermal system consists of an avoidable and an unavoidable part [42].

$$\dot{E}_{D,k} = \dot{E}_{D,k}^{AV} + \dot{E}_{D,k}^{UN} \tag{49}$$

The unavoidable part can be calculated by equation (50) [11]:

$$\dot{E}_{UN,k} = \dot{E}_{P,k} \left(\dot{E}_D / \dot{E}_P \right)_k^{UN} \tag{50}$$

The actual and unavoidable operating conditions of each component are summarized in Table 5.

Equation (51) defines the exergetic efficiency ϵ_k^* in the function of the avoidable destruction of exergy in the k-esimo [11].

$$\epsilon_k^* = \frac{\dot{E}_{P,k}}{\dot{E}_{F,k} + \dot{E}_{D,k}^{UN}} = 1 - \frac{\dot{E}_{D,k}^{AV}}{\dot{E}_{F,k} + \dot{E}_{D,k}^{UN}} \tag{51}$$

2.5.3. Combination of the parts

The two divisions endogenous/exogenous and avoidable/inevitable are combined and expressions for the terms avoidable-endogenous are obtained $(\dot{E}_{D,k}^{AV,EN})$, avoidable-exogenous $(\dot{E}_{D,k}^{AV,EX})$, inevitable-endogenous $(\dot{E}_{D,k}^{UN,EN})$ and inevitable-exogenous $(\dot{E}_{D,k}^{UN,EX})$ and are presented respectively in Equations (52)–(54) y 55 [40].

$$\dot{E}_{D,k}^{AV,EN} = \dot{E}_{P,k}^{EN} - \dot{E}_{D,k}^{UN,EN} \tag{52}$$

$$\dot{E}_{D,k}^{AV,EX} = \dot{E}_{P,k}^{EX} - \dot{E}_{D,k}^{UN,EX} \tag{53}$$

Table 5
Actual and unavoidable operating conditions of each plant component [11].

Component	Actual process	Inevitable process
CT	$\eta_s = 0.89$	$\eta_s = 0.95$
AH	$\epsilon = 0.2628$	$\epsilon = 0.3417$
HRSG	$\epsilon = 0.2326$	$\epsilon = 0.3023$
TGH	$\epsilon = 0.5027$	$\epsilon = 0.6536$
TGTH	$\epsilon = 0.2264$	$\epsilon = 0.2943$
CC	$\Delta T = 281.3^\circ K$	$\Delta T = 10K$
CONV	$Q = 26509 \text{ kJ/kg}$	$Q = 0$
ABS	$H_R = 0.67HR$	$H_P = 0.98HR$

$$\dot{E}_{D,k}^{UN,EN} = \dot{E}_{P,k}^{EN} \left(\frac{\dot{E}_D}{\dot{E}_P} \right)_k^{UN} \tag{54}$$

$$\dot{E}_{D,k}^{UN,EX} = \dot{E}_{P,k}^{UN} - \dot{E}_{D,k}^{UN,EN} \tag{55}$$

In the advanced exergo-economic analysis, the cost rates associated with exergy destruction, capital investment, operation, and maintenance are expressed in four categories: endogenous avoidable, exogenous avoidable, endogenous inevitable, and exogenous inevitable [10]. Table 6 shows the equations associated with the advanced exergo-economic analysis for each component.

2.6. Validation of the thermodynamic model

The objective of the thermodynamic model is to characterize the behavior of the nitric acid production plant. This model allows establishing the necessary analyses to determine the moles of the combustion processes of each of the reactive equipment. For the validation of the thermodynamic model, the data of the real molar flows of the plant production under normal operating conditions were used. In Tables 6–8 the moles of the products at the outlet of the CONV, CC, and ABS and the total production of nitric acid were compared, respectively, concerning the real products and real output of each plant component.

The most considerable difference in Table 7 was that of NO with a difference of 5 %, followed by O₂ with a difference of 2.7 %. The moles of H₂O did not show any difference between the results of the model and the real values. On the other hand, in Table 8, the enormous difference corresponds to the NO₂ + NO, followed by the HNO₃. In contrast, in Table 9 they were HNO₃ y H₂O respectively. Their difference could have been given because the plant works in real conditions while the parameters of the program validation operate in an ideal way. The chemical equilibrium equations mentioned above use logarithmic terms and therefore, the model is variable. There is a difference between the values of the real moles and the thermodynamic model’s moles because the moles of each compound is obtained both from the balance of actual moles of the plant and from the chemical equilibrium equations described in Ref. [35]. Likewise, the chemical equilibrium equations use logarithmic terms, and therefore the model is variable.

In turn, the difference in nitric acid production from the ideal model and the real production of real nitric acid, the error does not exceed 2.0511 %, whose percentage indicates that the thermodynamic model is useful. It is possible to observe that the differences obtained between the parameters compared were less than 5 %. These differences may be because some operating parameters do not have a measurement system to determine them during the operation of the nitric acid production plant. Therefore, adjustments were made to the different unknown values in the thermodynamic model to obtain results close to those obtained in the plant.

On the other hand, Fig. 3 shows the variation of ammonia concentration at the inlet to the gas mixer concerning the cooling temperature. It can be seen that the ammonia concentration decreases as cooling is achieved because the air density has an inverse

Table 6
Equations used for advanced exergo-economic analysis.

Term	Division of exergy destruction costs	Division of investment costs
Inevitable	$\dot{C}_{D,k}^{UN} = c_{f,k} \dot{E}_{D,k}^{UN}$	$\dot{Z}_{D,k}^{UN} = \dot{E}_{P,k} \left(\frac{\dot{E}_{D,k}}{\dot{E}_{P,k}} \right)^{UN}$
Avoidable	$\dot{C}_{D,k}^{AV} = c_{f,k} \dot{E}_{D,k}^{AV}$	$\dot{Z}_{D,k}^{AV} = \dot{Z}_k - \dot{Z}_{D,k}^{UN}$
Endogenous	$\dot{C}_{D,k}^{EN} = c_{f,k} \dot{E}_{D,k}^{EN}$	$\dot{Z}_{D,k}^{EN} = \dot{E}_{P,k}^{EN} \left(\frac{\dot{Z}_k}{\dot{E}_{P,k}} \right)^{Real}$
Exogenous	$\dot{C}_{D,k}^{EX} = c_{f,k} \dot{E}_{D,k}^{EX}$	$\dot{Z}_{D,k}^{EX} = \dot{Z}_k - \dot{Z}_{D,k}^{EN}$
Inevitable Endogenous	$\dot{C}_{D,k}^{UN,EN} = c_{f,k} \dot{E}_{D,k}^{UN,EN}$	$\dot{Z}_{D,k}^{UN,EN} = \dot{E}_{P,k}^{EN} \left(\frac{\dot{Z}_k}{\dot{E}_{P,k}} \right)^{UN}$
Evitable Endogenous	$\dot{C}_{D,k}^{AV,EN} = c_{f,k} \dot{E}_{D,k}^{AV,EN}$	$\dot{Z}_{D,k}^{AV,EN} = \dot{Z}_{D,k}^{EN} - \dot{Z}_{D,k}^{UN,EN}$
Inevitable Exogenous	$\dot{C}_{D,k}^{UN,EX} = c_{f,k} \dot{E}_{D,k}^{UN,EX}$	$\dot{Z}_{D,k}^{UN,EX} = \dot{Z}_{D,k}^{UN} - \dot{Z}_{D,k}^{UN,EN}$
Evitable Exogenous	$\dot{C}_{D,k}^{AV,EX} = c_{f,k} \dot{E}_{D,k}^{AV,EX}$	$\dot{Z}_{D,k}^{AV,EX} = \dot{Z}_{D,k}^{EX} - \dot{Z}_{D,k}^{UN,EX}$

Table 7
Results of the validation of the thermodynamic model at the CONV.

Compounds	Moles/hr Real	Moles/hr Thermodynamic Model	Difference (%)
H ₂ O	949.2	949.2	0
O ₂	389.2	400.4	2.7
N ₂	4189	4199	0.02
NO	522.4	493.4	5

Table 8

Results of the validation of the thermodynamic model in the CC.

Compounds		Moles/hr Reales	Moles/hr Thermodynamic	Difference (%)
O_2	194.1	198.5	2.26	
N_2	4189	4189	0	
$NO_2 + NO$	350.7	336.5	4.2	
HNO_3	171.8	175.9	2.3	
H_2O	863.2	851.3	1.3	

Table 9

Results of the validation of the thermodynamic model in the ABS.

Compounds	Moles/hr Reales	Moles/hr Thermodynamic	Difference (%)
H_2O	1456.4	1483	1.8
$NO_2 + NO$	0.3	0.285	5
HNO_3	509.2	498.76	2.05
Nitric acid production (Ton/day)		Model Nitric acid production (Ton/day)	Difference (%)
349.04		341.88	2.051

relationship with the weather as described in Equation (5).

From Fig. 4, it is possible to observe the variation of the concentration of the products of the combustion process in the CONV concerning the cooling temperature. It is observed that concentrations increase as cooling is achieved, this is because the air temperature in the intermediate stages of the TC presents an inverse relationship to the mass flow, which causes the moles of O_2 , N_2 , and H_2O entering the CONV to increase as cooling is achieved, leading to the products also increase.

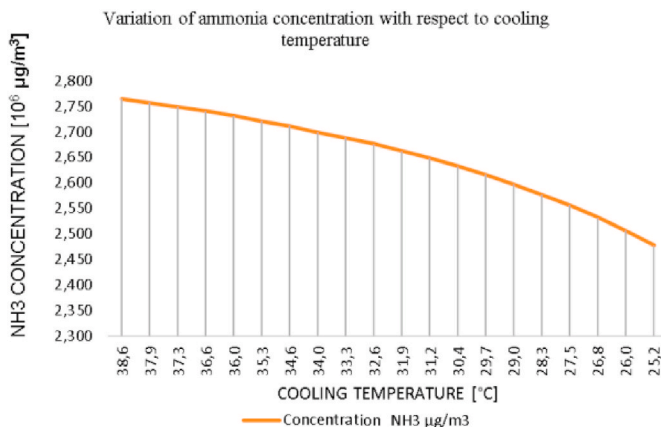
Meanwhile, Fig. 5 shows that the concentrations of O_2 , NO , H_2O , and N_2 that leave the CC increase as cooling is achieved; this is because the air temperature in the intermediate stages of the TC has an inverse relationship to the mass flow, causes the moles of the products at the CONV output to increase as shown in Fig. 6. These moles enter the CC, implying that the moles of the reagents at the CC input also increase, causing the products at the CC output to have the same upward behavior.

Fig. 6 shows that the concentrations of HNO_3 , H_2O , NO_2 , and NO coming out of the ABS increase as cooling is achieved. This is because the air temperature in the intermediate stages of the TC presents an inverse relationship to the mass flow, and therefore the moles of the products in the output of the CONV are increased as shown in Fig. 3; then these moles enter the CC, and then the moles of the reagents at the input and output in the ABS are also increased.

3. Results and discussion

3.1. Conventional exergetic and exergo-economic analysis

The results of the exergetic and exergo-economic analysis are summarized in Table 11, where it can be seen that the CONV has the highest exergetic destruction and the third lowest exergetic efficiency with 28202.33 kW and 47.69 %, respectively, in turn

**Fig. 3.** Variation of ammonia concentration concerning cooling temperature.

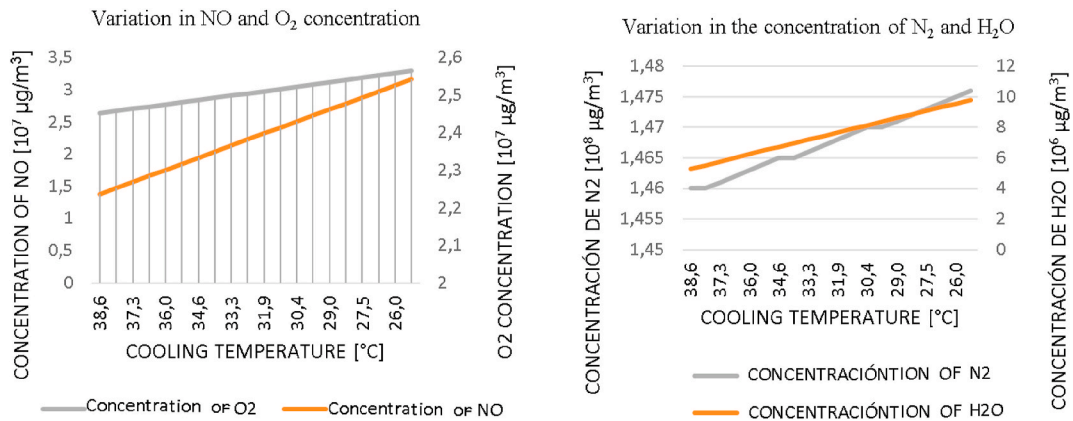


Fig. 4. Variation in the concentration of NO, N₂, O₂, and H₂O at the CONV outlet for the cooling temperature.

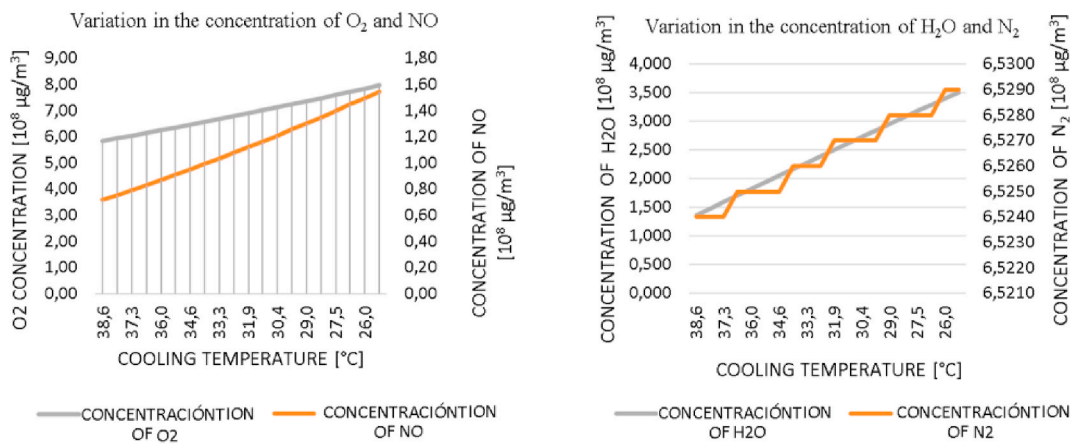


Fig. 5. Variation of the concentration of NO, N₂, O₂, and H₂O at the CC output concerning the cooling temperature.

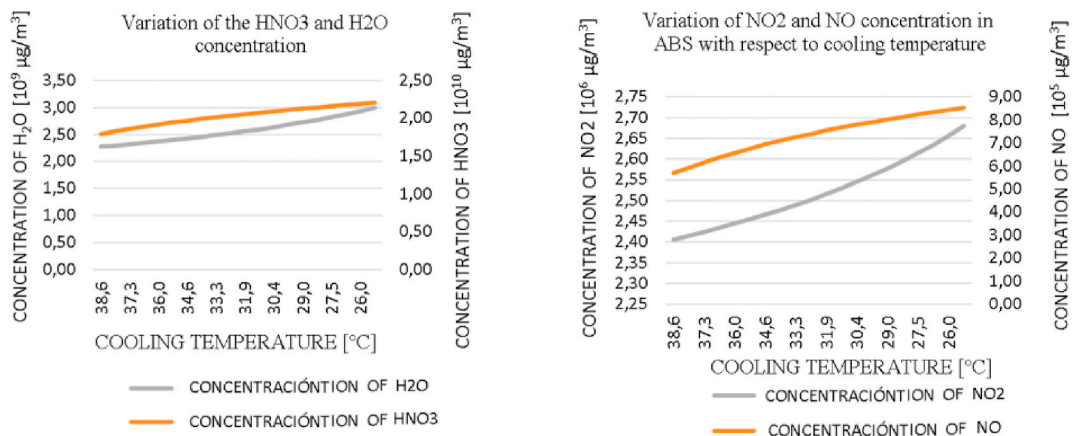


Fig. 6. Variation of the concentration of NO, N₂, O₂, and H₂O at the ABS output concerning the cooling temperature.

maintaining 58.80 % of the exergetic collapse of the entire system. The TGTH has the lowest exergetic efficiency of the system with 21.18 %, although its exergy destruction is also the lowest 152.34 kW. The heat exchanger network formed by the AH, HRS, TGH, and TGHT is the components that have less exergy destruction than the total exergy destroyed with 1.20 %, 1.73 %, 0.75 %, and 0.31 %, respectively.

While the exergo-economic analysis reveals that the total investment cost of the plant is 675,131 \$/h, with TGH being the

Table 10
Formulas for calculating the PEC of plant components.

Component	Purchased equipment costing functions
CT	Compressor HPC: $C_{HPC} = 7,90(HP)^{0.62}(k\$)$ [43] Compressor LPC $C_{LPC} = 7,90(HP)^{0.62}(k\$)$ [43]: Turbine (ST) $C_{ST} = 0,378(HP)^{0.81}(k\$)$ [43]: Expander (EXP): $C_{ST} = 0,378(HP)^{0.81}(k\$)$ [43]
CONV	$C_{CONV} = a + bS^n (\$)$ [44]
AH	$C_{AH} = a + bS^n (\$)$ [44]
HRSG	$C_{HRSG} = a + bS^n (\$)$ [44]
TGH	$C_{TGH} = a + bS^n (\$)$ [44]
TGTH	$C_{TGTH} = a + bS^n (\$)$ [44]
CC	$C_{CC} = a + bS^n (\$)$ [44]
ABS	$C_{ABS} = 1,218[f_1 C_b + Nf_2 f_3 f_4 C_t + C_{pr}] (\$)$ [43]

Table 11
Conventional exergetic and exergo-economic analysis of the nitric acid production plant.

Component	$\dot{E}_F (KW)$	$\dot{E}_P (KW)$	$\dot{E}_D (KW)$	$\langle i \rangle y_{D,k}^* (\%) \langle i \rangle$	$\langle i \rangle \epsilon (\%) \langle i \rangle$	$\dot{c}_{F,k} (\frac{\$}{GJ})$	$\dot{c}_{P,k} (\frac{\$}{GJ})$	$\dot{C}_{D,k} (\frac{\$}{h})$	$\dot{Z}_k (\frac{\$}{h})$	\dot{r}_k	$f_k (\%)$
CT	16046.74	3565.76	12480	25.14	22.22	8538	38421	106.56	167.09	3.50	61.06
CONV	53908.79	25706.5	28202	56.80	47.69	20670	26920	582.94	104.9	0.30	15.25
AH	1616.54	1018.43	598.1	1.20	63.00	7565	26015	4.52	14.331	2.44	76.00
HRSG	4117.13	3257.00	860.1	1.73	79.11	7565	9758	6.51	37.37	0.29	85.17
TGH	805.76	432.39	373.3	0.75	53.66	7565	14380	2.82	18.9	0.90	87.00
TGTH	193.28	40.93	152.3	0.31	21.18	7352	34716	1.12	111.71	3.72	99.01
CC	11385.16	10121.8	1263.3	2.54	88.90	2071	2497	2.62	69.1	0.21	96.35
ABS	9815	3689	6126	8.64	37.58	14840	15531	63.68	151.73	0.05	70.44

equipment with the highest associated investment cost, followed by ABS, with 167.09 \$/h and 151.73 \$/h respectively, from where we also denote that they are the most expensive equipment of the plant. While AH presents the lowest associated investment cost with 14,331 \$/h. The TC, TGTH, and AH have a higher relative cost different than the other components whose relative cost values range between 0.05 and 0.9.

The lowest exergoeconomic factor is presented in the CONV, therefore investments should be made in this component to reduce the costs of exergy destruction, taking into account that this component represents 56.8 % of the total exergy destruction. The highest values of the exergo-economic factor are for the TGTH (99.01 %), followed by the CC (96.35 %) and the Cola TGH (87 %). For these three types of equipment, it is beneficial to reduce the total investment to improve the economy of the process, even if it increases the cost of exergy destruction. The exergy destruction cost of the plant is \$770.77/hr. Table 10 describes the cost functions that were used to obtain the PEC of the plant components.

The Compression Train (CT), Tail Gas Desuperheater (TGTH), and Absorption Tower (ABS) have the lowest exergetic efficiencies compared to the others, as a result of irreversibilities in chemical reactions, fluid mixing non-homogenized, heat transfer to the environment, among others (Fig. 7).

Fig. 8 shows the distribution of heat transferred to the environment as a result of the energy balance, for a total transfer of 30176.76 KW. Where it can be seen that CT has the highest heat transfer, followed by ABS, while TGH is the equipment that transfers the least heat to the environment compared to the other components of the plant.

On the other hand, Fig. 9 shows the relationship between the total fuel exergy of the plant and the daily production of nitric acid concerning the cooling temperature where the fuel of the nitric acid production plant remains as a fixed value. This parameter corresponds to the exergy of the air, the exergy of water vapor entering the TC, the exergy of ammonia entering the CONV, and the exergy of cooling water entering the ABS. While the daily production of nitric acid varies concerning the cooling temperature. This ratio decreases because the concentration of nitric acid, leaving the ABS increases as cooling is achieved as shown in Fig. 5.

Continuing with the analysis of results from the conventional exergo-economic study, Fig. 10 shows the relationship of nitric acid cost and daily nitric acid production to the cooling temperature where the nitric acid cost remains fixed. In contrast, the nitric acid concentration increases as cooling is achieved, as shown in Fig. 7. The decrease in air temperature implies that the mass flow increases, which means an increase in nitric acid concentration, so it can be deduced that the air temperature reaching 25.22 °C causes the plant to achieve more excellent production than normal operating conditions.

3.2. Advanced exergetic analysis

The results of the advanced exergetic analysis, presented in Table 12, show that 54 % of the total exergetic destruction can be recovered by an intervention of the components. The CONV and CT are the components with the most significant potential for

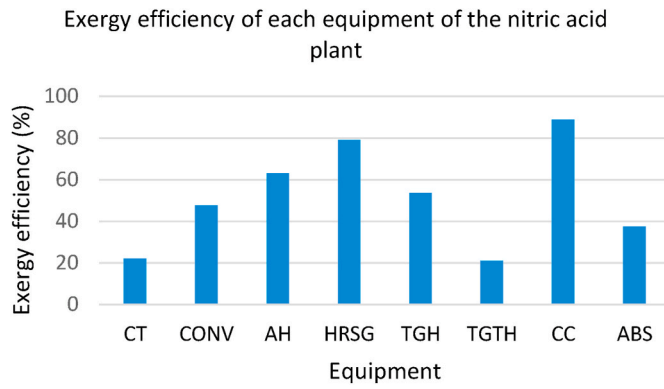


Fig. 7. Exergy efficiency of each piece of equipment of the nitric acid plant.

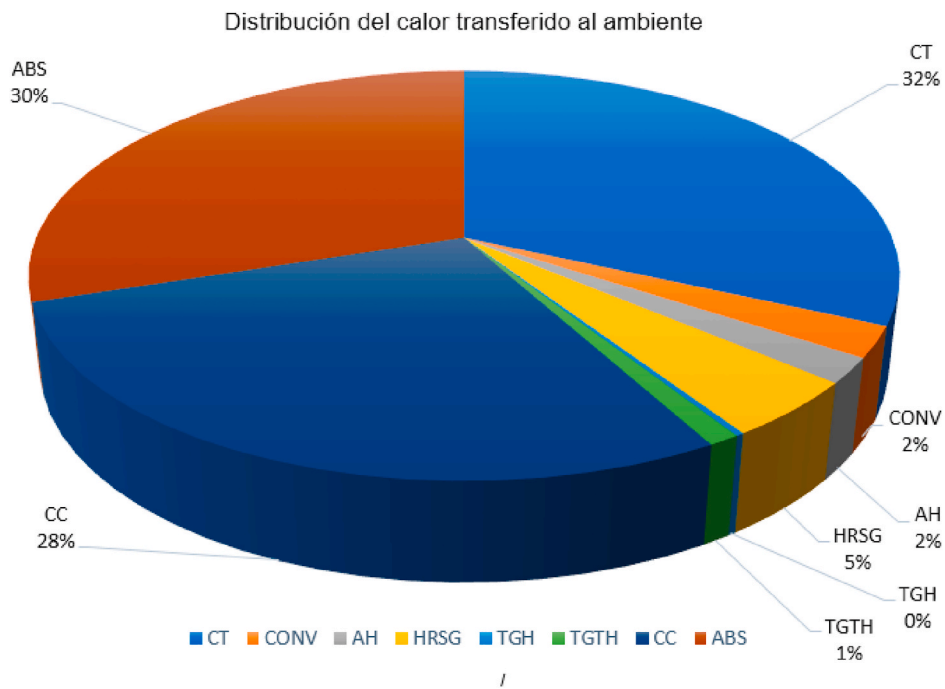


Fig. 8. Distribution of lost heat to the environment.

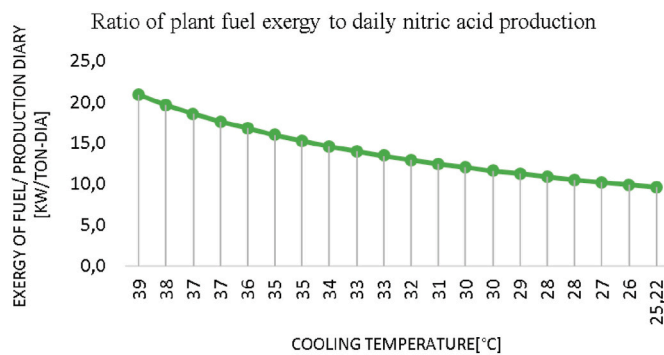


Fig. 9. The ratio of fuel exergy and daily nitric acid production to the cooling temperature.

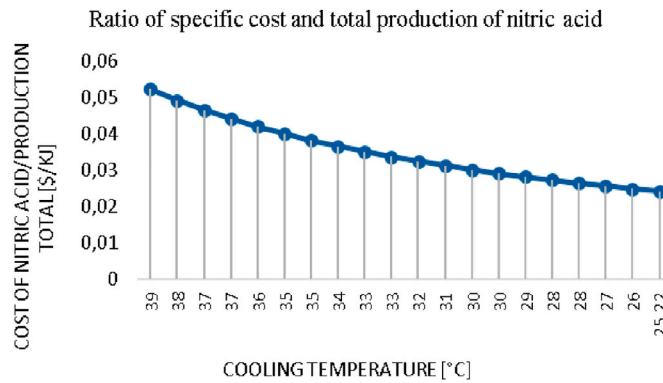


Fig. 10. Variation of specific cost ratio and total nitric acid production for cooling temperature.

improvement with 75 % and 11 %, respectively of the total avoidable exergy destruction. In the same way, it can be seen that approximately 51 % of exergy destruction is due to the malfunctioning of the components themselves [45], and 49 % of plant irreversibility is due to the interaction between the members. The TC presents the highest irreversibility caused by the operation of the other plant equipment with 75 % of its exergy destruction, followed by the CONV with approximately 30 % of its exergy destruction.

According to Table 12, the CC, TGTH, HRSF, and TGTH are the components with the least improvement potential with 0.3 %, 0.3 %, 0.5 %, and 1 %, respectively, while ABS has an improvement potential of 9.5 % to the plant’s improvement potential. In the same way, Table 13 presents the results of the advanced exergetic analysis after the plant reached the cooling temperature.

3.3. Advanced exergo-economic analysis

The investment cost associated with CONV’s avoidable exergy destruction is 54.4 \$/h. This means that more than 50 % of the total cost of your exergy destruction can be reduced by improving the other plant equipment’s performance. While the exogenous investment cost rate \dot{Z}_k^{EX} of the TC represents 66.2 % of the total investment cost. 85 %, 88 %, and 83 % of the investment cost of the TGTH, ABS, and CONV, respectively, is exogenous, that is, it is only affected by the structure of the plant and the functioning of the other components, but not by its internal thermodynamic inefficiencies. It is inferred that the exogenous investment cost rate, \dot{Z}_k^{EX} is higher than the endogenous cost rate, $\dot{Z}_{i,k}^{EN}$ for most of the plant’s components, so the interactions between the components significantly affected investment costs.

Table 14 shows the endogenous, exogenous, avoidable, and unavoidable exergetic costs of each plant component, while Table 15 shows the investment costs associated with advanced exergetic economic analysis.

4. Conclusions

The present study allowed the implementation of a methodology to characterize thermodynamically all the components of the plant. The results obtained in the validation process show that the implemented method can be used as a useful tool to develop advanced exergo-economic analyses to nitric acid production plants as the one studied in this work, guaranteeing that the results obtained with the model can be used as references for other researches of the scientific community. This methodology can be extrapolated to different plant configurations.

The implemented methodology allowed deducing that the endogenous exergy of the plant is 51 %, which indicates that exergy is destroyed mainly by the components’ irreversibilities and not by the interaction among them. The inevitable exergy destruction is

Table 12
Destruction of inevitable, avoidable, endogenous, and exogenous exergy of each of the components of the plant.

Component	$\dot{E}_D(KW)$	$\dot{E}_D^{UN}(KW)$	$\dot{E}_D^{AV}(KW)$	$\dot{E}_D^{EN}(KW)$	$\dot{E}_D^{EX}(KW)$	$\dot{E}_D^{AV,EN}(KW)$	$\dot{E}_D^{AV,EX}(KW)$	$\dot{E}_D^{UN,EN}(KW)$	$\dot{E}_D^{UN,EX}(KW)$
CT	12480	9255	3216	2576	9452.98	2263.54	510.43	312.45	8942.54
CONV	28202	7608	20594	19628	8574.33	19549.18	1045.14	78.81	7529.18
AH	598.11	157.3	440.8	374.2	223.91	365.35	75.45	8.84	148.45
HRSF	860.13	716.6	143.5	138.8	721.43	121.32	22.30	17.47	699.12
TGH	373.36	112.7	260.7	77.86	295.5	72.24	188.41	5.61	107.08
TGTH	152.34	74.9	77.44	5.827	146.513	1.97	75.46	3.85	71.04
CC	1263.32	1174	89.22	52.7	1210.62	41.70	47.61	10.99	1163.00
ABS	6126	3126	2594	2283	3843	2248.07	751.92	34.92	3091.07
Total	50056	22224	27832	25136.	24468.28	24663.38	2716.79	473.00	21751.50

Table 13

Inevitable, avoidable, endogenous, and exogenous exergy destruction of each of the plant components at an air inlet temperature of 25.22 °C.

Component	$\dot{E}_D (KW)$	$\dot{E}_D^{UN} (KW)$	$\dot{E}_D^{AV} (KW)$	$\dot{E}_D^{EN} (KW)$	$\dot{E}_D^{EX} (KW)$
CT	11768	11134	634	10120	1648
CONV	13599	10344	3255	12351	1248
AH	368.5	210.1	158.4	302	48.5
HRSG	602.8	540	62.8	58	544.8
TGH	322	89.9	232.1	102.4	219.6
TGTH	133.2	92.3	40.9	8.45	124.75
CC	1784	952.4	831.6	710	1074
ABS	6126	2671	3455	3090	3036

Table 14

Endogenous, exogenous, avoidable, and unavoidable exergetic costs of each plant component.

Component	$\dot{C}_{Dk} (\frac{\$}{h})$	$\dot{C}_{Dk}^{EN} (\frac{\$}{h})$	$\dot{C}_{Dk}^{EX} (\frac{\$}{h})$	$\dot{C}_{Dk}^{AV} (\frac{\$}{h})$	$\dot{C}_{Dk}^{UN} (\frac{\$}{h})$	$\dot{C}_{Dk}^{AVEN} (\frac{\$}{h})$	$\dot{C}_{Dk}^{AVEX} (\frac{\$}{h})$	$\dot{C}_{Dk}^{UNEN} (\frac{\$}{h})$	$\dot{C}_{Dk}^{UNEX} (\frac{\$}{h})$
CT	106.56	102.6	3.96	98.7	7.86	66.46	120.2	96.04	95.76
CONV	582.94	550.4	32.54	494.8	88.14	491.5	266.19	58.65	58.08
AH	4.52	4.34	0.18	1.2	3.32	4.1	3.57	2.41	2.37
HRSG	6.51	1.9	4.61	3.901	2.609	1.48	2.56	4.76	45.70
TGH	2.82	2.58	0.24	0.79	2.03	1.53	1.58	1.53	1.56
TGTH	1.12	0.43	0.69	0.2	0.92	0.43	5.827	1.02	1.37
CC	2.62	1.7	0.92	1.6	1.02	1.68	1.85	0.82	72.07
ABS	63.68	63.5	0.18	13.8	49.88	44.89	42.65	18.66	18.49

Table 15

Division of investment cost rates for plant components.

Component	$\dot{z}_k (\frac{\$}{h})$	$\dot{z}_k^{EN} (\frac{\$}{h})$	$\dot{z}_k^{EX} (\frac{\$}{h})$	$\dot{z}_k^{AV} (\frac{\$}{h})$	$\dot{z}_k^{UN} (\frac{\$}{h})$	$\dot{z}_k^{AVEN} (\frac{\$}{h})$	$\dot{z}_k^{AVEX} (\frac{\$}{h})$	$\dot{z}_k^{UNEN} (\frac{\$}{h})$	$\dot{z}_k^{UNEX} (\frac{\$}{h})$
CT	167.09	56.35	110.74	19.6	147.5	6.59	13.0	49.76	97.74
CONV	104.9	17.78	87.12	54.4	50.46	5.28	49.2	12.5	37.96
AH	14.331	8.08	6.251	3.9	10.4	2.2	1.7	5.88	4.52
HRSG	37.37	2.97	34.4	1.3	36.1	0.09	1.2	2.88	33.22
TGH	18.9	3.40	15.5	6.1	12.8	1.1	5.0	2.30	10.5
TGTH	111.71	15.90	95.81	44.8	66.9	6.37	38.4	9.53	57.37
CC	69.1	5.8	63.3	8.9	60.2	0.6	8.3	5.2	55
ABS	151.73	16.95	134.78	41.2	110.5	6.75	34.5	10.2	100.3

22224.5 kW, which represents 44.4 % of the total exergy destruction. Likewise, most of the exergy destruction (55.6 %) can be recovered by performing an intervention in the components; the CONV and the CT have the highest and the lowest potential for improvement to the other parts of the plant respectively, whose avoidable exergy destruction is 20594 kW and 3216 kW respectively.

In the heat exchanger network, the components' investment costs can be reduced because when cooling is achieved, the exergonomic factor increases by up to 11, 5, and 1.7% points in the AH, HRSG, and TGH, respectively. On the other hand, the CONV's exergonomic factor increases by 11 % when cooling is achieved, so the investment costs of this component must be taken into account to complete the reduction of exergy destruction costs.

The interactions between the components significantly affected the investment costs. The total exergy destruction cost of the CONV represents 75 % of the full plant exergy destruction cost and can be reduced by improving the other equipment's performance.

Credit author statement

Ana Buevas Hernández: Software EES, Writing- Original manuscript and revisions versions, simulations.

Juan Gabriel Fajardo: Conceptualization, Methodology, Supervision.

Deibys Barreto: Methodology, simulations, Supervision.

Gaylord Carrillo Caballero: Visualization, Editing, Investigation.

Yulineth Cárdenas Escorcía: Visualization, Reviewing, revisions versions.

Carlos Ramón Vidal Tovar: Reviewing and Editing

Yimy Gordon Hernández: Conceptualization and Editing

Conflicts of interest statement

The authors whose names are listed immediately below certify that they have NO affiliations with or involvement in any organization or entity with any financial interest (such as honoraria; educational grants; participation in speakers' bureaus; membership, employment, consultancies, stock ownership, or other equity interest; and expert testimony or patent-licensing arrangements), or non-financial interest (such as personal or professional relationships, affiliations, knowledge or beliefs) in the subject matter or materials discussed in this manuscript.

Declaration of competing interest

The authors declare that they have no known competing financial interests or personal relationships that could have appeared to influence the work reported in this paper.

Acknowledgments

To the Universidad Tecnológica de Bolívar for providing all the necessary resources to carry out this study.

References

- [1] K. Iftekhar, F. Alam y, Q. Alam, The global climate change and its effect on power generation, *Energy Pol.* (2013) 1460–1470.
- [2] R. Rivero, Application of the exergy concept in the petroleum refining and petrochemical industry, *Energy Convers. Manag.* 43 (2002) 1199–1220.
- [3] A. Valero, M.A. Lozano, M. Muñoz, A General Theory of Exergy Saving I, II and III, ASME, New York, 1986.
- [4] A. Bejan, G. Tsatsaronis y, M. Moran, *Thermal Designing and Optimization*, New York, John Wiley & Sons, 1996.
- [5] P. Ifaei, A. Ataei y, C. Yoo, Thermo-economic and environmental analyses of a low water consumption combined steam power plant and refrigeration chillers- Part 2: thermo-economic and environmental analysis, *Energy Convers. Manag.* 123 (2016) 625–642.
- [6] C. Yan, L. Lv, S. Wei, A. Eslamimanesh, W. Shen, Application of retrofitted design and optimization framework based on the exergy analysis to a crude oil distillation plant, *Appl. Therm. Eng.* 154 (2019) 637–649.
- [7] O.J. Odejebi, Exergy and economic analyses of crude oil distillation unit, *Afr. J. Eng. Res.* 3 (2015) 44–55.
- [8] K. Altayib, I. Dincer, Analysis and assessment of using an integrated solar energy-based system in a crude oil refinery, *Appl. Therm. Eng.* 159 (2019) 12.
- [9] Z. Nur Izyan y, M. Shuhaimi, Exergy analysis for fuel reduction strategies in crude distillation unit, *Energy* 66 (2014) 801–807.
- [10] D. Barreto, J. Fajardo y, J. Campillo, Determination of the optimal range of the compressor inlet air temperature in a power plant with stig cycle through of advanced exergetic analysis, de ASME Int. Mechan. Eng. Congr. Exposit., Proc., Salt Lake City 6 (2019). *Energy*.
- [11] A. Buelvas, H. Valle y, J. Fajardo, Avoidable and unavoidable exergetic destruction analysis of a nitric acid production plant, de ASME 2018 Int. Mechan. Eng. Congr. Exposit., Pennsylvania 6B (2018). *Energy*.
- [12] L. Tock, F. Marechal, Co-production of hydrogen and electricity from lignocellulosic biomass: process design and thermo-economic optimization, *Energy* 45 (2012) 339–349.
- [13] P. Caliandro, L. Tock, A.V. Ensinas, F. Marechal, Thermo-economic optimization of a solid oxide fuel cell- gas turbine system fuelled with gasified lignocellulosic biomass, *Energy Convers. Manag.* 85 (2014) 764–773.
- [14] D. Brown, M. Gassner, T. Fuchino, F. Maréchal, Thermo-economic analysis for the optimal conceptual design of biomass gasification energy conversion systems, *Appl. Therm. Eng.* 29 (2009) 2137–2152.
- [15] M. Rivarolo, B. D. M. A, A. Massardo, Hydro-methane and methanol combined production from hydroelectricity and biomass: thermo-economic analysis in Paraguay, *Energy Convers. Manag.* 79 (2014) 74–84.
- [16] G. Singh, P. Singh, V. Tyagi, P. Barnwal, A. Pandey, Exergy and thermo-economic analysis of ghee production plant in the dairy industry, *Energy* 167 (2019) 602–618.
- [17] A. Abusoglu, M. Kanoglu, Exergetic and thermo-economic analyses of diesel engine powered cogeneration: Part 2 – Application, *Appl. Therm. Eng.* 29 (2009) 242–249.
- [18] X. Zhang, R. Zeng, K. Mu, X. Liu, X. Sun, H. Li, Exergetic and exergoeconomic evaluation of co-firing biomass with natural gas in CCHP system integrated with ground source heat pump, *Energy Convers. Manag.* 180 (2019) 622–640.
- [19] S. Seyyedi, M. Hashemi-Tilehnoe, M.A. Rosen, Exergy and exergoeconomic analyses of a novel integration of a 1000 MW pressurized water reactor power plant and a gas turbine cycle through a superheater, *Ann. Nucl. Energy* 115 (2018) 161–172.
- [20] L. Castellon, J. Fajardo, B. Sarria, Thermo-economic analysis of wheat flour agroindustrial planta, in: *Proceedings of the 15 the International Mechanical Engineering Congress and Exposition*, Texas, Houston, 2015.
- [21] M. Bin Shams, E. Elkanzi, Z. Ramadhan, S. Rahma y, M. Khamis, Gas turbine inlet air cooling system for enhancing propane recovery in a gas plant: theoretical and cost analyses, *Nat. Gas Sci. Eng.* (2017) 34.
- [22] M. Callak, F. Balkan, A. Hepbalsi, Avoidable and unavoidable exergy destructions of a fluidized bed coal combustor and heat recovery steam generator, *Energy Convers. Manag.* 98 (2015) 54–58.
- [23] H. Nami, A. Nemat, F.J. Fard, Conventional and advanced exergy analyses of a geothermal driven dual fluid organic Rankine cycle (ORC), *Appl. Therm. Eng.* (2017) 46.
- [24] O. Balli, Advanced exergy analyses to evaluate the performance of a military aircraft turbojet engine (TJE) with afterburner system: splitting exergy destruction into unavoidable/avoidable and endogenous/exogenous, *Appl. Therm. Eng.* 111 (2017) 152–169.
- [25] M. Yari, S.M. Mahmoudi, M. Fallah, Advanced exergy analysis for an anode gas recirculation solid oxide fuel cell, *Energy* 141 (2017) 1097–1112.
- [26] Z. Wang, W. Xion, D.S.-K. Ting, R. Carrière, Z. Wang, Conventional and advanced exergy analyses of an underwater compressed air energy storage system, *Appl. Energy* 180 (2016) 810–822.
- [27] S. Fellaou, T. Bounahmidi, Analyzing thermodynamic improvement potential of a selected cement manufacturing process: advanced exergy analysis, *Energy* 154 (2018) 190–200.
- [28] A. Pazildar y, S. Sadrameli, Conventional and advanced exergoeconomic analyses applied to ethylene refrigeration system of an existing olefin plant, *Energy Convers. Manag.* 138 (2017) 474–485.
- [29] A. Palizdar, T. Ramezani, Z. Nargessi, S. AmirAfshar, M. Abbasi, A. Vatani, Advanced exergoeconomic evaluation of a mini-scale nitrogen dual expander process for liquefaction of natural gas, *Energy* 168 (2019) 542–557.
- [30] M. Mehrpooya, H. Ansarinassab, Advanced exergoeconomic evaluation of single mixed refrigerant natural gas liquefaction processes, *J. Nat. Gas Sci. Eng.* 26 (2015) 782–791.
- [31] M. Mehrpooya, S. Ali Mousavi, Advanced exergoeconomic assessment of a solar-driven Kalina cycle, *Energy Convers. Manag.* 178 (2018) 78–91.
- [32] H. Ansarinassab, M. Mehrpooya, M. Pouriman, Advanced exergoeconomic evaluation of a new cryogenic Helium recovery process from natural gas based on the flash separation - APCI modified process, *Appl. Therm. Eng.* 132 (5) (2017) 368–380.

- [33] D. Barreto, J. Fajardo, G. Carrillo y, Y. Cardenas, Advanced and exergoeconomic analysis of a gas power system with steam injection and air cooling with a compression refrigeration machine, *Energy Technol.* 9 (2021) 16.
- [34] Y. Cengel, *Termodinámica*, Mexico, 2011.
- [35] S. Turn, *An introduction to combustion concepts and application*, 2000.
- [36] A. Buelvas, J. Fajardo y, H. Valle, Conventional and advanced exergoeconomic analysis in a nitric acid production plant, *Int. Mech. Eng. Congr. Exposit., Salt Lake City* 6 (2020). *Energy*.
- [37] J. Egzergia Szargut, *Poradnik obliczania I stosowania*, Editor: wydawnictwo politechniki shlaskej, Gliwice, 2007, 129 pages.
- [38] A. Abusoglu y, M. Kanoglu, Exergetic and thermoeconomic analyses of diesel engine powered, *Appl. Therm. Eng.* 29 (2008) 234–241.
- [39] A. Bejan, G. Tsatsaronis y, M. Moran, *Thermal Design & Optimization*, JOHN WILEY & SONS, INC, Toronto, 1996.
- [40] L. Wang, Y. Yang, T. Morosuk y, G. Tsatsaronis, Advanced thermodynamic analysis and evaluation of a supercritical power plant, *Energies* 5 (2012) 1850–1863.
- [41] G. Tsatsaronis, K. Solange y, T. Morosuk, Endogenous and exogenous exergy destruction in thermal systems, in: *Proceedings of International Mechanical Engineering Congress and Exposition-IMECE*, vol. 2006, 2006, pp. 311–317.
- [42] G. Tsatsaronis y, M. Park, On Avoidable and unavoidable exergy destructions and investment costs in thermal systems, *Energy Convers. Manag.* 43 (2002) 1259–1270.
- [43] J. Couper, W. Penney, J. Fair y, S. Walas, *Chemical Process Equipment: Selection and Design*, Butterworth-Heinemann, 2010.
- [44] G. Towler y, R. Sinnott, *Chemical Engineering Design: Principles, Practice, and Economics of Plant and Process Design*, Butterworth-Heinemann, 2013.
- [45] J. Fajardo, H. Valle, A. Buelvas, Avoidable and unavoidable exergetic destruction analysis of a nitric acid production plant, *ASME Int. Mech. Eng. Congr. Exposit., Pittsburgh* 6B (2018). *Energy*.